Proc. Natl. Acad. Sci. USA
Vol. 80, pp. 1207–1211, March 1983
Biochemistry

Synthesis of aspartate transcarbamoylase in *Escherichia coli*: Transcriptional regulation of the *pyrB–pyrI* operon

(promoter/attenuation/leader peptide/S1 nuclease mapping)

MARC NAVRE AND H. K. SCHACHMAN*

Department of Molecular Biology and Virus Laboratory, Wendell M. Stanley Hall, University of California, Berkeley, California 94720

Contributed by Howard K. Schachman, November 29, 1982

ABSTRACT **The first committed reaction in pyrimidine biosynthesis in *Escherichia coli* and *Salmonella typhimurium* is catalyzed by the allosteric enzyme aspartate transcarbamoylase (aspartate carbamoyltransferase; carbamoylphosphate:L-aspartate carbamoyltransferase, EC 2.1.3.2), the product of the *pyrB–pyrI* operon. Regulation of the pyrimidine pathway is achieved in part by changes in the enzyme's catalytic activity as a function of the concentration of substrates and other metabolites as well as by variations in enzyme synthesis in response to changes in cellular levels of pyrimidine nucleotides. Although there is substantial evidence that UTP concentration has a marked influence on expression of the *pyrB–pyrI* operon, the mechanism of this control is not known. We have cloned the operon and determined the nucleotide sequence of the region preceding the first structural gene (*pyrB*). These studies show two regions sharing considerable homology with the consensus sequence of *E. coli* promoters, a segment that can code for a 44-amino-acid leader peptide, and a sequence very similar to that of the attenuator of the *trp* operon. RNA transcripts from several bacterial strains were studied by S1 nuclease mapping. Under conditions leading to extensive enzyme synthesis there was a large production of transcript whose 5′ end correlated with the putative promoter closer to the structural genes. At low levels of operon expression there was little transcript in the extracts and both promoters appeared to serve as initiation sites. The results are interpreted in terms of transcriptional control of the *pyrB–pyrI* operon according to an attenuation model that differs in novel ways from the mechanisms proposed for the regulation of amino acid biosynthesis.**

Pyrimidine synthesis in *Escherichia coli* and *Salmonella typhimurium* is regulated in part by the allosteric enzyme aspartate transcarbamoylase (ATCase; aspartate carbamoyltransferase; carbamoylphosphate:L-aspartate carbamoyltransferase, EC 2.1.3.2), which catalyzes the first committed step in the biosynthetic pathway. Control is achieved in several ways. The enzyme itself regulates the formation of carbamoyl aspartate through the sigmoidal dependence of catalytic activity on the concentration of both substrates (1, 2). Also, ATCase is inhibited by CTP, the end product of the pyrimidine pathway, and activated by ATP (1). In addition to the regulation provided by the allosteric properties of ATCase, control is achieved at the level of protein synthesis. ATCase production is relatively low at high levels of UTP, a product of the pyrimidine biosynthetic pathway, whereas enzyme synthesis is increased as much as 150-fold when the cellular concentration of UTP is very low (3). The mechanism of regulation of the synthesis of ATCase is not known.

The catalytic and regulatory chains of *E. coli* ATCase are encoded by the *pyrB* and *pyrI* genes, respectively (4). Recent studies of deletion mutants and molecular cloning experiments followed by nucleotide sequence analysis showed that the *pyrB* and *pyrI* genes constitute an operon with the two contiguous genes separated by a 15-nucleotide, untranslated, intercistronic region (4). One *pyrB* deletion produced a normal amount of regulatory chains even though a substantial portion of the *pyrB* gene was removed. Another deletion, which shares a similar end point within *pyrB*, produced no regulatory polypeptide chain because of the removal of the promoter region (4). These results indicated that a single region adjacent to *pyrB* controls transcription of both *pyrB* and *pyrI*. Recently Roof *et al.* (5), on the basis of their nucleotide sequence determination of the promoter region, suggested that attenuation and other "overlapping" regulatory mechanisms were implicated in the control of the *pyrB–pyrI* operon. In an independent study, Turnbough *et al.* (6) determined the sequence of the 620 nucleotides preceding the *pyrB* structural gene. Also, they demonstrated by *in vitro* transcription experiments the presence of a UTP-dependent pause site and interpreted their results in terms of attenuation control (6). We have determined the nucleotide sequence of the promoter region from two genetically distinct sources of DNA and have characterized the *in vivo* transcripts from strains in which the intracellular levels of pyrimidine nucleotides were varied. The attenuator model presented here is similar to that of Turnbough *et al.* (6) and is analogous to those proposed for the regulation of operons involved in amino acid biosynthesis (7, 8).

MATERIALS AND METHODS

Bacterial Strains and Media. Both *E. coli* and *S. typhimurium* strains were used in these studies. The episome F393 *argF lac proAB* (P22 *pyrB*) was derived from specialized transduction of *pyrB* into *F128 argF lac proAB* of *E. coli* K-12 (9). F393 carries the intact *pyrB–pyrI* operon and its regulatory elements (4). Mutation *pyrH700* encodes a partially defective UMP kinase. Strains carrying this mutation have decreased levels of UDP and UTP and as a result overproduce ATCase (10, 11). Mutation *pyrB655* is a deletion that removes all of *pyrB* (12). Because *pyrB655* and *pyrH700* are available only in *S. typhimurium*, we have employed a hybrid organism in which the *pyrB–pyrI* operon from *E. coli* is present in *S. typhimurium* (4, 9, 13). The *E. coli* strain AT2535 carrying the *pyrB59* allele (4) was used in the selection of transformants maintaining *pyrB*$^+$ plasmids. When uracil was used in the growth medium for the various bacterial strains, the concentration was 20 μg/ml.

Plasmid Construction. Conditions for restriction endonuclease digestions and ligation reactions, as well as plasmid purification and transformation techniques, were described earlier

The publication costs of this article were defrayed in part by page charge payment. This article must therefore be hereby marked "*advertisement*" in accordance with 18 U. S. C. §1734 solely to indicate this fact.

Abbreviations: ATCase, aspartate transcarbamoylase; kb, kilobase(s); bp, base pair(s).

* To whom reprint requests should be addressed.

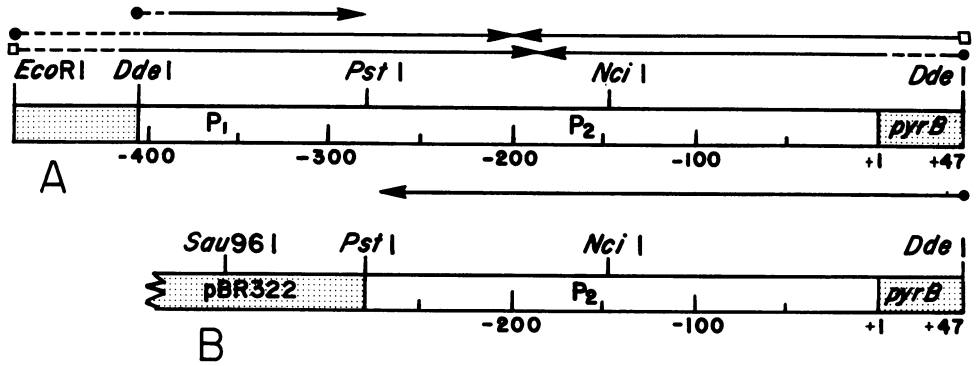

FIG. 1. Restriction maps of segments of *pyrB–pyrI* plasmids and strategy for determining nucleotide sequence. (*A*) Promoter region of plasmid pPYRB3, which contains a 3.0-kb *Eco*RI/*Sal* I insert derived from F393. The diagram shows the segment of pPYRB3 from the *Eco*RI site to a *Dde* I site 47 bp past the ATG of the *pyrB* gene. Sequences are numbered from the ATG start codon of the *pyrB* gene with the A as +1 and the base preceding it as −1. Arrows above the map indicate the direction and extent of sequence determined for each fragment. Dashed portions of the arrows represent segments that were not observed on the sequencing gels. Fragments were labeled on either their 5′ (●) or 3′ (□) ends as described in the text. The arrow below the map represents the single-stranded *Pst* I/*Dde* I fragment used as a hybridization probe for the transcript mapping experiment. P_1 and P_2 designate the two transcriptional promoters encoded on the insert (see text). The shaded region between the *Eco*RI site and the *Dde* I site at −420 represents the section of F393 DNA that was not derived originally from the *pyrB* region of the *E. coli* chromosome. (*B*) Restriction map of the promoter region of pPYRB9. This plasmid contains only P_2. The *Pst* I site at −285 is the junction between the insert derived from the λ phage yk14m5 and the vector DNA. Sequences are numbered as in *A*.

(4). Two different DNAs were used for the construction of plasmids containing the *pyrB–pyrI* operon. The 4.8-kilobase (kb) plasmid, pPYRB9, is a subclone derived from pDP8 (unpublished results). Plasmid pDP8 contains the *pyrB* gene from the λ specialized transducing phage yk14m5 (4). A second plasmid, pPYRB3, of 6.7 kb contains a 3.0-kb *Eco*RI/*Sal* I fragment from F393 inserted into pBR322 (unpublished).

Sequence Determination. DNA was labeled at its 5′ or 3′ termini (4), and nucleotide sequences were determined by the method of Maxam and Gilbert (14) as modified by Smith and Calvo (15).

Analysis of *in Vivo* *pyrB–pyrI* Transcripts. *S. typhimurium* strains HS2343 (*argI2002 fol-101 leuD798 proAB47 pyrB655 pyrH700*/pPYRB3) and HS2351 (*fol-101 leuD798 pyrB655*/pPYRB3) were grown to midlogarithmic phase and RNA was isolated by extraction with hot phenol (16). DNA remaining in the RNA preparations was removed by incubating the solution with iodoacetate-treated DNase I followed by passing the digest through a nitrocellulose filter (G. Christie, personal communication). The mixture was then extracted with phenol and the RNA was precipitated with ethanol.

A single-stranded, end-labeled DNA hybridization probe was prepared by labeling the 5′ ends of the 455-base-pair (bp) fragment produced by digesting pPYRB3 with *Dde* I. After secondary digestion with *Pst* I, the fragment was purified and the strands were separated by the procedure of Maxam and Gilbert (14). Various RNA preparations were hybridized (17, 18) to the single-stranded DNA probe as follows: 200 μg of RNA was mixed with 1 μg of the hybridization probe, and the solution was heated to 70°C for 10 min, followed by incubation at 53°C for 3 hr. The DNA·RNA hybrids were treated with 350 units of S1 nuclease (Boehringer Mannheim) for 30 min at 25°C and then for 15 min at 0°C. The samples were precipitated with ethanol and analyzed on a denaturing polyacrylamide gel in parallel with a set of sequencing reactions performed on the double-stranded, end-labeled fragment.

Assay of ATCase Activity in Crude Extracts. Cultures of HS1053 (AT2535/pPYRB3) and HS1057 (AT2535/pPYRB9) were grown in minimal media to midlogarithmic phase and crude extracts were prepared by the freeze–thaw protocol of Jenness (19) and assayed for ATCase activity (20). Protein concentrations were determined with bovine serum albumin as a standard.

RESULTS

Nucleotide Sequence of the *pyrB–pyrI* Promoter. Both pPYRB3 and pDP8 promote the synthesis of catalytic and regulatory chains of ATCase when used to transform cells carrying the *pyrB655* deletion. The precise location of the *pyrB* and *pyrI* genes in pPYRB3 was determined by comparing the results of restriction mapping with the sequence of *pyrB–pyrI* from plasmid pDP8 (21). Fig. 1*A* shows the relevant portion of pPYRB3 containing the promoter and the 5′-terminal region of *pyrB*; the analogous region of pPYRB9 is shown in Fig. 1*B*. The strategy used for determining the nucleotide sequence of the 420 bp on the 5′ side of the *pyrB* gene in pPYRB3 is illustrated in Fig. 1*A*. This sequence, shown in Fig. 2, is the same as that of the equivalent promoter region studied by Turnbough *et al.* (6) and the corresponding region of pPYRB9 (unpublished results).

Various features of the sequence in Fig. 2 are relevant. First, the region at −165, containing the sequence T-A-T-A-A-T-G, is identical to the consensus sequence of the −10 site (Pribnow box) of *E. coli* promoters (22). The T-T-G at −190 corresponds to the consensus sequence for the −35 site of the promoter. Hence the region at −165, designated P_2 to be consistent with the nomenclature used by Turnbough *et al.* (6), could be a promoter with the initiation of transcription at −155. Downstream from this putative promoter, at −145, is a G-G-A-G-G sequence, followed 4 bp later by an ATG. This sequence corresponds with known consensus sequences for initiation of translation (23). As seen in Fig. 2, the ATG codon starting at −138 could encode the beginning of a 44-amino-acid leader peptide,† which is terminated at the codon TAA located at −6 bp from the start of the *pyrB* structural gene.

The second relevant structural feature of the DNA sequence is the large region of dyad symmetry at −108 to −86, followed by a pyrimidine-rich sequence. This inverted repeat can form a hairpin in the transcript with an estimated free energy of −15 kcal/mol (24) (1 kcal = 4.18 kJ). Analogous hairpins have been observed in studies of the control of the *trp* operon and have been shown to cause transcriptional pausing *in vitro* (25, 26). Although it is tempting to designate this hairpin at −108 to −86 a transcriptional pause site, it is important to note (27)

† Our sequence differs slightly from that of Roof *et al.* (5), whose results predict a 43-amino-acid leader peptide.

```
      -410       -400       -390       -380       -370       -360       -350       -340       -330       -320       -310       -300
GCACCTTCCT TAGCCGTTCG CTTTCACACT CCGCCCTATA AGTCGGATGA ATGGAATAAA ATGCATATCT GATTGCGTGA AAGTGAAAAA GGAAAAAGCA GGGAATGTCT GCAATTATTG

      -290       -280       -270       -260       -250       -240       -230       -220       -210       -200       -190       -180
ATACCGAAGG ACAGTTCCCC TGCAGAATCA CATCAAATAA AAATGCATAT ACCTTGACTT TTAATTCAAA TAAACCGTTT GCGCTGACAA AATATTGCAT CAAATGCTTG CGCCGCTTCT

      -170       -160       -150       -140       -130       -120       -110       -100        -90        -80
GACGATGAGT ATAATGCCGG ACAATTTGCC GGGAGGATGT ATG GTT CAG TGT GTT CGA CAT TTT GTC TTA CCG CGT CTG AAA AAA GAC GCT GGC CTG CCG TTT TTC
                                  MET VAL GLN CYS VAL ARG HIS PHE VAL LEU PRO ARG LEU LYS LYS ASP ALA GLY LEU PRO PHE PHE

-70        -60        -50        -40        -30        -20        -10         +1
TTC CCG TTG ATC ACC CAT TCC CAG CCC CTC AAT CGA GGG GCT TTT TTT TGC CCA GGC GTC AGG AGA TAA AAG ATG GCT
PHE PRO LEU ILE THR HIS SER GLN PRO LEU ASN ARG GLY ALA PHE PHE CYS PRO GLY VAL ARG ARG *** MET ALA
```

FIG. 2. Nucleotide sequence of the *pyrB–pyrI* regulatory region of pPYRB3. Numbering is that indicated in Fig. 1. Bases underlined around −410 bp represent the junction between *E. coli* chromosomal DNA and F393 DNA. Also underlined are the nucleotide sequences corresponding to P_1, P_2, and the leader peptide ribosomal binding site (see text). The potential 44-amino-acid leader peptide is indicated below the nucleotide sequence. The sequence of *pyrB* begins at +1 with the codons corresponding to methionine and alanine.

that such hairpins are not always pause sites. Hence, the demonstration by Turnbough *et al.* (6) that pausing does occur *in vitro* at this site at low UTP levels is of particular interest.

A third significant region of the DNA sequence is the dyad repeat at −49 to −32 followed by eight Ts. This region, which is very similar to the *trp* attenuator of *E. coli* (8), satisfies the structural requirements for ρ-independent transcription termination sites (28).

Finally, there is a sequence at −360 bp from the start of *pyrB* which shows some homology to the *E. coli* promoter consensus sequence. Evidence that this structure, designated P_1 by Turnbough *et al.* (6), serves *in vivo* as a functional promoter is presented below.

S1 Nuclease Mapping of *pyrB–pyrI* Transcripts. In an effort to provide information about the regulation of *pyrB–pyrI* transcription *in vivo* we performed S1 nuclease mapping with RNA isolated from two strains of *S. typhimurium* containing the plasmid pPYRB3. Transcripts from strain HS2343 carrying the *pyrH700* mutation are representative of expression of the *pyrB–pyrI* operon under conditions that lead to overproduction of ATCase. In contrast, the *pyrH*$^+$ strain HS2351 provides data for expression under conditions leading to lower levels of ATCase synthesis, which can be varied by growing the cells in the presence or absence of uracil.

The transcripts were analyzed by hybridizing the cellular RNAs to the single-stranded *Pst* I/*Dde* I fragment of pPYRB3 that was labeled at the 5′ terminus (Fig. 1*A*) and treating the heteroduplex mixture with S1 nuclease to digest the single-stranded region of the *Pst* I/*Dde* I fragment not protected by the *pyrB–pyrI* transcript.‡ Fig. 3 shows the results of the S1 nuclease mapping experiments along with the fragments generated by the chemical sequence analysis reactions. The fragments protected by RNA from HS2343 are shown in lane 1. The positions of these bands indicate that the 5′ end of the transcript corresponds to the sequence A-T-T-T at −155, which is 9 bp downstream from P_2. Because of the imprecision of the technique, we could not determine uniquely the nucleotide at the 5′ end of the transcript. Lanes 2 and 3 show the fragments protected by RNA from HS2351 grown, respectively, in the presence and absence of uracil.

The results show that the strain carrying the *pyrH700* mutation produces the largest amount of *pyrB–pyrI* transcript. Moreover, at the low levels of UTP in this strain, more than 95% of the transcript derives from P_2. In contrast, the *pyrH*$^+$ strain produces only a small amount of *pyrB–pyrI* transcript, with slightly more being made when the cells were grown in the absence of uracil. It should be noted that a small amount of the single-stranded probe remains undigested in lanes 1–3. Transcripts initiated before the *Pst* I site of the promoter region, possibly at P_1, could have protected this fragment from digestion.

Deletion of P_1. The availability of two clones of *pyrB–pyrI*, pPYRB3 and pPYRB9, provided an opportunity to evaluate features essential to the regulation of the operon. Inspection of Fig. 1 indicates that pPYRB9 does not contain P_1. Despite this difference, the results in Table 1 indicate that strains containing either plasmid exhibited the change in *pyrB–pyrI* expression usually observed at varying levels of uracil. It is interesting to note, however, that the amount of ATCase produced in HS1053 (carrying both P_1 and P_2) was somewhat greater than that in HS1057 (carrying P_2 only).

DISCUSSION

Transcriptional Regulation of ATCase Synthesis. By using specially constructed mutants of *S. typhimurium* that permit manipulation of various pyrimidine nucleotide pools, Schwartz and Neuhard obtained evidence indicating that UTP was in-

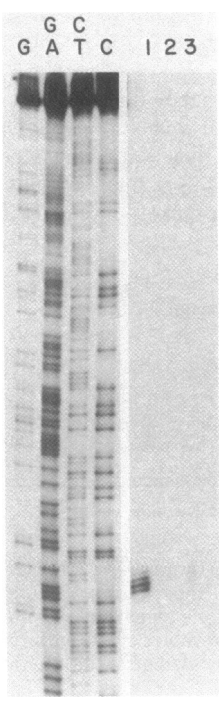

FIG. 3. Hybridization analysis of *pyrB–pyrI* transcripts. The first four lanes represent nucleotide sequences of the double-stranded *Pst* I/*Dde* I fragment corresponding to the arrow at the bottom of Fig. 1*A*. The lanes numbered 1–3 were derived by hybridization of the single-stranded probe shown in the bottom of Fig. 1*A* to cellular RNA from HS2343 (lane 1) and HS2351 grown in the presence (lane 2) or absence (lane 3) of uracil, followed by S1 nuclease digestion (see text). The products were analyzed by electrophoresis on a denaturing 5% polyacrylamide gel. Lanes 1–3 were exposed to film approximately 5 times longer than the sequence analysis lanes. The autoradiograms were obtained from the same gel.

‡ In this mapping experiment the labeled DNA fragment was digested to the point in the promoter sequence corresponding to the 5′ end of the transcript. The location of this site was determined by comparing the size of the digested DNA with the sizes of those fragments generated by the sequencing reactions (14). Corrections were made for the difference in migration of the fragments generated by S1 nuclease and the corresponding fragments produced by chemical cleavage (29).

Table 1. Activity of ATCase in various strains

Strain	Relevant genotype	Specific activity* Uracil present	Specific activity* Uracil absent	Ratio of activities
HS1053	*pyrB59*/pPYRB3	13	90	7
HS1057	*pyrB59*/pPYRB9	2.8	20	7

* Activities are expressed as μmol of carbamoyl aspartate formed per hr per mg of protein in the crude extract.

volved in regulating the synthesis of ATCase (3). In this regard, strains that produce a partially defective UMP kinase due to a leaky *pyrH* mutation are particularly useful because they produce a 30- to 75-fold increase in ATCase synthesis relative to isogeneic *pyrH*$^+$ strains (3, 9). It was of interest, therefore, to determine whether the amount of RNA transcribed from the *pyrB–pyrI* operon could be correlated with the production of ATCase. As shown by the S1 nuclease mapping experiments in Fig. 3, the amount of transcript produced in strain HS2343 carrying the *pyrH700* mutation is greatly increased over that in the *pyrH*$^+$ strain HS2351 grown in the presence or absence of uracil. Moreover, the amount of transcript in strain HS2351 was larger when these cells were grown in the absence of uracil. Such *pyrH*$^+$ strains generally show a 2- to 7-fold increase in the synthesis of ATCase when grown in the absence of uracil as compared to the same cells when supplemented with uracil (ref. 3 and Table 1).

Although quantitative data for the amounts of transcript are lacking, these results provide a qualitative correlation between the amounts of *pyrB–pyrI* transcript and of ATCase produced under the various growth conditions. Thus, the results are consistent with the view that synthesis of ATCase is under transcriptional control.

Identification of Promoter Sites. As seen in Fig. 2, the nucleotide sequence of the 418 bases upstream from the *pyrB* structural gene in pPYRB3 contains a region at −165 corresponding to the consensus sequence of *E. coli* promoters (22). In addition to this potential site (P_2 in Fig. 1) for the initiation of transcription, there is a second site, P_1, which, as judged on the basis of its nucleotide sequence, also could function as a promoter. As shown by Turnbough *et al.* (6), both of these sites serve *in vitro* as initiation sites for transcription. In the light of these observations the S1 nuclease mapping experiments are of particular interest.

It is clear from the results in Fig. 3 that P_2 does function *in vivo* as a promoter. Moreover, at high levels of *pyrB–pyrI* expression (in the *pyrH700* strain) more than 95% of the *in vivo* transcript originates from P_2 (lane 1). Only a small amount of transcript is detected from the region corresponding to P_1. Lanes 2 and 3 show, however, that comparable amounts of transcript originate from P_1 and P_2 when there is a low level of *pyrB–pyrI* expression (in a *pyrH*$^+$ background). Additional evidence that both P_1 and P_2 serve as promoters *in vivo* is seen in Table 1. Strain HS1053, which contains both promoters in plasmid pPYRB3, produced greater amounts of ATCase than strain HS1057, which contains plasmid pPYRB9 from which P_1 is deleted.

The results with strain HS1057 indicate that P_1 is not required for changes in expression of the operon at varying levels of uracil. Nonetheless it is possible that P_1 may be implicated in constitutive synthesis of ATCase at low expression of *pyrB–pyrI*. When the level of expression is high, however, most of the transcription originates from P_2. Control mechanisms of this type with two promoters have been described for the *trp* system (30).

Model for the Regulation of *pyrB–pyrI* Expression. Although our understanding of the expression of the *pyrB–pyrI* operon is meager in comparison to that for the regulation of amino acid biosynthetic operons (7, 8), the limited data presented above are sufficient to justify the suggestion of an analogous attenuator model for the regulation of the *pyrB–pyrI* operon. In addition to the transcriptional promoters, P_1 and P_2, there is a segment that can code for a leader peptide. Included in the 3′ end of the coding region for the leader peptide is the attenuator structure that can serve as a transcription terminator. Also, the transcript can form a stable secondary structure from −108 to −86, as shown in Fig. 4, and could function as the UTP-dependent pause site invoked by Turnbough *et al.* (6).

According to the model, transcription is initiated by the binding of RNA polymerase to P_1, P_2, or both. At high cellular UTP levels, transcription proceeds until the polymerase reaches the transcription terminator 30 bp before the start of the *pyrB* gene. Under these conditions, the hairpin of the attenuator will form, transcription will terminate, and there will be no expression of *pyrB–pyrI*. When the UTP concentration is low, however, the polymerase pauses at about −80, just beyond the hairpin shown in Fig. 4 (6). As a result of this pausing, there is time for a ribosome to bind to the transcript and initiate the synthesis of the leader peptide shown in Fig. 2. As proposed by Winkler and Yanofsky (25), transcriptional pausing facilitates the synchronization of transcription and translation that is required in attenuator-regulated systems. The pausing at low UTP concentration would allow the ribosome to "catch up" with the paused polymerase and, upon continuation of transcription, prevent formation of the RNA hairpin of the attenuator at −49 to −32. As a consequence, termination of transcription would not occur, and the entire *pyrB–pyrI* operon would be transcribed. Thus, at low cellular concentration of UTP there would be a high level

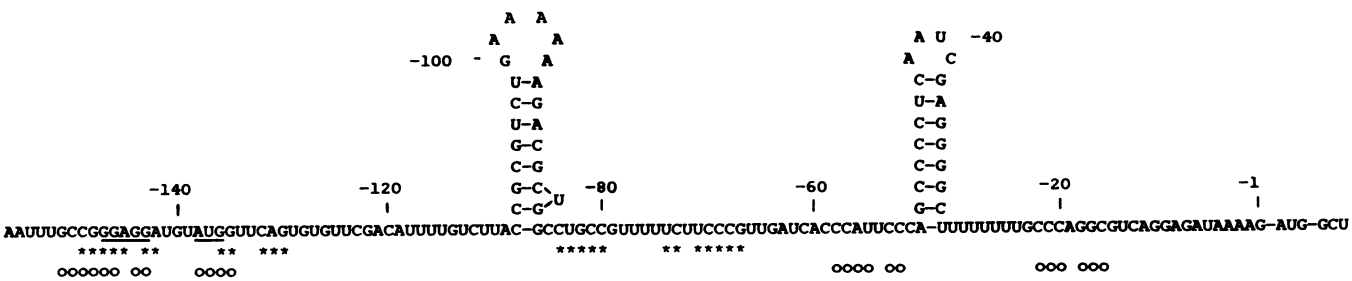

FIG. 4. Potential secondary structures in the *pyrB–pyrI* transcript. The hairpins indicated are the most stable structures that can form, as judged on the basis of thermodynamic parameters. The transcript is numbered in the same fashion as Fig. 1*B*. Base-pairing structures that can form between the leader peptide ribosomal binding site region and the promoter distal portions of the attenuated transcript (*) or read-through transcript (o) are shown below the RNA sequence. The values of ΔG for formation of the secondary structures are −15 kcal/mol for the hairpin at −110 to −80, −21 kcal/mol for the attenuator, −19 kcal/mol for the attenuated transcript interaction (*), and −29 kcal/mol for the read-through transcript interaction (o).

of expression of the *pyrB–pyrI* operon and overproduction of ATCase.

In addition to the hairpins shown in Fig. 4, other stable secondary structures can be formed by base pairing between nucleotides near the attenuator stem loop and those located around the ribosomal binding site and initiator codon of the leader peptide. These interactions, which can occur when there is either termination of transcription or read-through to the structural genes of the operon, are similar to those described by Yanofsky (8) for the *trp* operon and may prevent repeated synthesis of the leader peptide.

Despite the similarities between the model proposed here and the models invoked earlier (7, 8) for the control of the operons implicated in amino acid biosynthesis, there are significant differences. The amino acid composition of the leader peptide, which is of special importance for the latter, does not appear to be relevant for the control of the *pyrB–pyrI* operon. It is the pausing of RNA polymerase due to low levels of UTP that is crucial for preventing attenuation of expression of *pyrB–pyrI*, rather than the stalling of the ribosome due to amino acid starvation that is involved in the regulation of the amino acid operons. Also, it is of interest that the coding region for the leader peptide in *pyrB–pyrI* operon extends beyond the attenuator site very close to the beginning of the structural gene; in other operons the coding region is substantially shorter and terminates before the attenuator.

The results presented here and the evidence from the *in vitro* transcription experiments of Turnbough *et al.* (6) support the view that regulation of the *pyrB–pyrI* operon is achieved by attenuation. The recent observation of Jensen *et al.* (31) that a mutation in *rpoB* or *rpoC* is responsible for constitutive synthesis of ATCase in a strain of *S. typhimurium* is also consistent with the attenuator model. As shown by Yanofsky and Horn (32), mutations in the *E. coli rpoB* gene result in strains with altered efficiencies in termination of transcription.

Additional tests of the attenuator model are clearly needed. Experiments are required to evaluate the role of P_1 *in vivo* and the effect of a two-promoter system. Moreover, it is necessary to determine whether the efficiency of transcription termination *in vivo* is sufficiently high to account for the 150-fold increase in ATCase synthesis at very low levels of cellular UTP. In view of the lack of positive evidence for a repressor protein and the ability of the attenuator model to account for changes in the synthesis of ATCase under various conditions of cell growth, we conclude that attenuation plays a principal role in regulating expression of the *pyrB–pyrI* operon.

We thank Gail Christie for many useful discussions and introducing us to the S1 nuclease technique, and we thank Charles Turnbough, who was kind enough to send us an early version of his manuscript and to share his findings with us. We thank James Wild for sending a copy of his paper prior to publication. We also thank Michael Karels for his advice and critical evaluation of our work. This research was supported by National Institute of General Medical Sciences Research Grant GM 12159 and by National Science Foundation Research Grant PCM80-23012.

1. Gerhart, J. C. & Pardee, A. B. (1962) *J. Biol. Chem.* **237**, 891–896.
2. Bethell, M. R., Smith, K. E., White, J. S. & Jones, M. E. (1968) *Proc. Natl. Acad. Sci. USA* **60**, 1442–1449.
3. Schwartz, M. & Neuhard, J. (1975) *J. Bacteriol.* **121**, 814–822.
4. Pauza, C. D., Karels, M. J., Navre, M. & Schachman, H. K. (1982) *Proc. Natl. Acad. Sci. USA* **79**, 4020–4024.
5. Roof, W. D., Foltermann, K. F. & Wild, J. R. (1982) *Mol. Gen. Genet.* **187**, 391–400.
6. Turnbough, C. L., Jr., Hicks, K. L. & Donahue, J. P. (1983) *Proc. Natl. Acad. Sci. USA* **80**, 368–372.
7. Johnston, H. M., Barnes, W. M., Chumley, F. G., Bossi, L. & Roth, J. R. (1980) *Proc. Natl. Acad. Sci. USA* **77**, 508–512.
8. Yanofsky, C. (1981) *Nature (London)* **289**, 751–758.
9. Jenness, D. D. & Schachman, H. K. (1980) *J. Bacteriol.* **141**, 33–40.
10. O'Donovan, G. A. & Gerhart, J. C. (1972) *J. Bacteriol.* **109**, 1085–1096.
11. Justesen, J. & Neuhard, J. (1975) *J. Bacteriol.* **123**, 851–854.
12. Syvanen, J. M. & Roth, J. R. (1973) *J. Mol. Biol.* **76**, 363–378.
13. Jenness, D. D. & Schachman, H. K. (1983) *J. Biol. Chem.* **258**, 3266–3279.
14. Maxam, A. & Gilbert, W. (1980) *Methods Enzymol.* **65**, 499–560.
15. Smith, D. R. & Calvo, J. M. (1980) *Nucleic Acids Res.* **8**, 2255–2274.
16. Salser, W., Gesteland, R. F. & Bolle, A. (1967) *Nature (London)* **215**, 588–591.
17. Berk, A. J. & Sharp, P. A. (1978) *Proc. Natl. Acad. Sci. USA* **75**, 1274–1278.
18. Barry, G., Squires, C. & Squires, C. L. (1980) *Proc. Natl. Acad. Sci. USA* **77**, 3331–3335.
19. Jenness, D. D. (1980) Dissertation (Univ. of California, Berkeley, CA).
20. Pastra-Landis, S. C., Foote, J. & Kantrowitz, E. R. (1981) *Anal. Biochem.* **118**, 358–363.
21. Pauza, C. D. (1981) Dissertation (Univ. of California, Berkeley, CA).
22. Rosenberg, M. & Court, D. (1979) *Annu. Rev. Genet.* **13**, 319–353.
23. Stormo, G. D., Schneider, T. D. & Gold, L. M. (1982) *Nucleic Acids Res.* **10**, 2971–2996.
24. Tinoco, I., Jr., Borer, P. N., Dengler, B., Levine, M. D., Uhlenbeck, O. C., Crothers, D. M. & Gralla, J. (1973) *Nature (London) New Biol.* **246**, 40–41.
25. Winkler, M. E. & Yanofsky, C. (1981) *Biochemistry* **20**, 3738–3744.
26. Farnham, P. J. & Platt, T. (1981) *Nucleic Acids Res.* **9**, 563–577.
27. Kingston, R. E. & Chamberlin, M. J. (1981) *Cell* **27**, 523–531.
28. Christie, G. E., Farnham, P. J. & Platt, T. (1981) *Proc. Natl. Acad. Sci. USA* **78**, 4180–4184.
29. Sollner-Webb, B. & Reeder, R. H. (1979) *Cell* **18**, 485–499.
30. Horowitz, H. & Platt, T. (1982) *J. Mol. Biol.* **156**, 257–267.
31. Jensen, K. F., Neuhard, J. & Schack, L. (1982) *EMBO J.* **1**, 69–74.
32. Yanofsky, C. & Horn, V. (1981) *J. Bacteriol.* **145**, 1334–1341.